NeuroImage: Clinical 12 (2016) 852–857

Contents lists available at ScienceDirect

NeuroImage: Clinical

journal homepage: www.elsevier.com/locate/ynicl

Identification of the stria medullaris thalami using diffusion tensor imaging☆,☆☆

Ryan B. Kochanski, MD[a], Robert Dawe, PhD[b,c], Daniel B. Eddelman, MD[a], Mehmet Kocak, MD[d], Sepehr Sani, MD[a,*]

[a]Department of Neurosurgery, Rush University Medical Center, 1725 W. Harrison St, Suite 855, Chicago, IL 60612, United States
[b]Rush Alzheimer's Disease Center, 600 S Paulina St, Chicago, IL 60612, United States
[c]Johnston R Bowman Health Center, 600 S Paulina St, Chicago, IL 60612, United States
[d]Department of Radiology, Rush University Medical Center, 1725 W. Harrison St, Suite 437, Chicago, IL 60612, United States

ARTICLE INFO

Article history:
Received 1 August 2016
Received in revised form 13 October 2016
Accepted 23 October 2016
Available online 26 October 2016

Keywords:
Diffusion tensor imaging (DTI)
Deep brain stimulation (DBS)
Depression
Stria medullaris (SM)

ABSTRACT

Background: Deep brain stimulation (DBS) via anatomical targeting of white matter tracts defined by diffusion tensor imaging (DTI) may be a useful tool in the treatment of pathologic neurophysiologic circuits implicated in certain disease states like treatment resistant depression (TRD). We sought to determine if DTI could be used to define the stria medullaris thalami (SM), the major afferent white matter pathway to the lateral habenula (LHb), a thalamic nucleus implicated in the pathophysiology of TRD.

Methods: Probabilistic DTI was performed on ten cerebral hemispheres in five patients who underwent preoperative MRI for DBS surgery. Manual identification of the LHb on axial T1 weighted MRI was used for the initial seed region for tractography. Variations in tractography depending on chosen axial slice of the LHb and chosen voxel within the LHb were also assessed.

Results: In all hemispheres the SM was reliably visualized. Variations in chosen axial seed slice as well as variations in single seed placement did not lead to significant changes in SM tractography.

Conclusions: Probabilistic DTI can be used to visualize the SM which may ultimately provide utility for direct anatomic targeting in DBS surgery.

1. Introduction

Advances in neuroimaging, along with a greater understanding of pathophysiology of neurophysiologic circuits, have led to the continued investigation of new targets for deep brain stimulation (DBS). Several targets have been implicated in treatment resistant depression (TRD) including subgenual cingulate cortex (SCC), nucleus accumbens (NAcc), ventral capsule/ventral striatum (VA/VS), lateral habenula (LHb), inferior thalamic peduncle (ITP), and the medial forebrain bundle (MFB) (Bewernick and Schlaepfer, 2013; Malone et al., 2009; Holtzheimer et al., 2012; Lozano et al., 2008; Sartorius and Henn, 2007; Coenen et al., 2011). More recently, the use of diffusion tensor imaging (DTI) based fiber tracking has heightened interest in anatomical targeting of white matter tracts that have been implicated in disease states like TRD (Schoene-Bake et al., 2010; Anthofer et al., 2015). Stimulation of the supero-lateral branch of the medial forebrain bundle (slMFB), a white matter tract that interconnects various centers of the reward pathway including the NAcc, ventral tegmental area (VTA), hypothalamus, and amygdala has shown promising results in the treatment of TRD and has spurred interest in the identification and stimulation of other white matter tracts involved in the pathophysiology of TRD (Coenen et al., 2009, 2011, 2012).

The stria medullaris thalamus (SM) is the major afferent pathway to the LHb, a small nucleus located on the dorsomedial surface of the caudal thalamus, adjacent to the third ventricle (Zhao et al., 2015). The habenular complex consists mainly of the lateral and medial components. The LHb receives input from a variety of limbic sources, in particular the septal region, NAcc, dorsomedial thalamus, and internal globus pallidus (GPi) (Zhao et al., 2015). Over activation of the LHb has been implicated in the downregulation of serotonergic, noradrenergic and dopaminergic activity as well as stimulation of the HPA axis (Sartorius and Henn, 2007; Sartorius et al., 2010). To date, DBS of the LHb has been described in only two patients but with promising results (Schneider et al., 2013). Because of its size and location, direct targeting of the LHb, although feasible, requires meticulous planning to both effectively target the structure and avoid side effects (Schneider et al.,

☆ Disclosure of funding: this research did not receive any specific grant from funding agencies in the public, commercial, or not-for-profit sectors.
☆☆ Financial support and industry affiliations: none.
* Corresponding author.
E-mail address: Sepehr_Sani@rush.edu (S. Sani).

http://dx.doi.org/10.1016/j.nicl.2016.10.018

2013). For this reason, broader targeting of the SM, a structure not visible on conventional MRI, may be more suitable for DBS surgery; however, to our knowledge, DTI-based fiber tracking of the SM has yet to be described. Here, we describe and assess the reliability of a technique using MRI-based probabilistic tractography to identify the SM which could in turn be used for direct targeting during DBS surgery.

2. Materials and methods

2.1. Subjects

Subjects were five consecutive patients undergoing pre-operative imaging for DBS surgery to treat Parkinson's disease. The subjects provided informed consent before enrolling in this study, which was approved by the Institutional Review Board of the authors' institution.

2.2. Image acquisition

Pre-operative MRI was carried out one to two weeks in advance of the scheduled DBS implantation procedure using a 3 T scanner and a 12-channel head coil (Siemens Magnetom Verio, Siemens Healthcare, Erlangen, Germany). No stereotactic frame was in place at the time of MRI, as our DBS workflow includes fusion of the MR images with CT images acquired the morning of surgery.

The routine pre-DBS MRI protocol includes a localizer, thin-slice T_2-weighted turbo spin echo sequences in the axial and coronal planes, a 3D gradient echo sequence for susceptibility-weighted imaging (SWI), and a post-contrast 3D T1-weighted sequence (MPRAGE) used for neuro-navigation. In the current work, the MPRAGE images were used as a reference for motion and distortion correction of diffusion images and were acquired using the following parameters: TR = 1.9 s, TE = 2.89 ms, TI = 900 ms, flip angle = 9°, bandwidth = 170 Hz/pixel, a parallel imaging (GRAPPA) acceleration factor of 2.0, 208 axial slices with thickness 1.2 mm, field of view 227.5 mm × 260 mm, acquisition matrix 224 × 256, yielding 1.02 mm × 1.02 mm in-plane resolution that was upsampled to 0.51 mm × 0.51 mm using the scanner's built-in interpolation option. The scan time was 3 min, 54 s.

For the purposes of this study, we also acquired a diffusion-weighted sequence prior to administration of contrast agent, with the following scan parameters: TR = 12.5 s, TE = 90 ms, flip angle = 90°, bandwidth = 1698 Hz/pixel, a parallel imaging acceleration factor of 3.0 to mitigate susceptibility distortions, 65 contiguous axial slices with thickness 2 mm to provide whole brain coverage (acquired in an interleaved fashion), field of view 256 mm × 256 mm, acquisition matrix 128 × 128, yielding isotropic 2 mm × 2 mm × 2 mm voxel dimensions. Using an EPI read-out, we acquired this data with a diffusion weighting factor (b-value) of 1000 s/mm^2 along 69 directions that were uniformly distributed in 3D space according to an electrostatic repulsion scheme (Jones et al., 1999), plus 8 acquisitions with no applied diffusion weighting. The scan time was approximately 16 min.

2.3. Data processing

Anonymized DICOM images were transferred to an offline workstation and converted to Neuroimaging Informatics Technology Initiative (NIfTI, .nii) format using the 'dcm2niigui' tool (Rorden et al., 2007). We deskulled the MPRAGE volume using FSL's 'bet' module, then imported all images, including the diffusion-weighted data, into TORTOISE (Pierpaoli et al., 2010), a software package for correction of motion, eddy current artifacts, and susceptibility distortions in the diffusion data using a high resolution structural image as a reference (the deskulled MPRAGE in this case) (Smith, 2002). Diffusion images were also upsampled to 1.5 mm × 1.5 mm × 1.5 mm by TORTOISE. Visual inspection of the corrected images revealed superb alignment of the diffusion-weighted data to the anatomic reference image and satisfactory mitigation of distortions, particularly in the thalamic and epithalamic regions, which were of greatest interest in the current work due to our targeting of the SM. We inspected all images for signs of motion artifacts warranting the discarding of individual images prior to tractography, but found none.

2.4. Probabilistic tractography

Although we first explored the use of deterministic tractography to highlight fibers of the SM, this technique proved sensitive to the choice of seed size and location in this particular application (see Supplement A). We therefore turned to probabilistic tractography as a potentially more robust means of guarding against aberrations arising from slight inconsistencies in seed placement. To this end, we first employed FSL's 'bedpostx' module to obtain distributions of diffusion parameters, including the principal diffusion direction, diffusivity, and diffusion anisotropy, for each voxel, using essentially the default settings. We chose to use a tool that allows for multiple fiber orientations because we expected there would often be axons from different fiber populations adjacent to and sometimes occupying the same voxels as the SM, which could greatly confound tractography of a white matter bundle as narrow as our target (Behrens et al., 2007).

Because the LHb most prominently receives input from other brain regions via the SM, we hypothesized that this small nucleus could serve as an opportune seed region for probabilistic tractography. Though its internal structure and contrast with adjacent tissue is limited at 3 T, the habenula can be reliably identified by its morphology on typically three consecutive 1.2-mm axial slices of the T1-weighted MPRAGE, in which it appears as a triangular ridge extending into the third ventricle on the medial surface of the thalamus (Lawson et al., 2013; Savitz et al., 2011; Strotmann et al., 2014). This visibility enabled us to manually draw a two-dimensional seed region within the habenula on its most central axial slice of the original, high-resolution MPRAGE images (Fig. 1). A single operator drew seeds for all subjects (ten total seed regions) in FSL's 'fslview' module (Jenkinson et al., 2012), maintaining a one-voxel spacing from the perceived interface between tissue and cerebrospinal fluid. Each seed included approximately 20 voxels.

We then carried out probabilistic tractography using FSL's 'probtrackx' module, with the results of bedpostx and the habenular seed region (left and right treated as separate cases) serving as inputs and utilizing essentially the default settings (Behrens et al., 2007). We

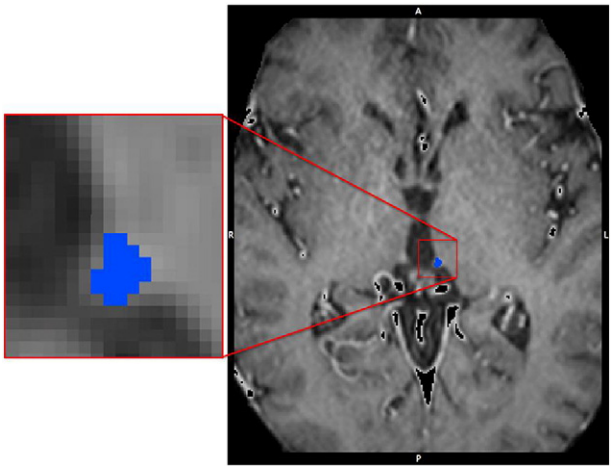

Fig. 1. Seeding the habenula. Tractographic identification of the SM requires a seed region from which candidate tracts project. Our seeding strategy initially consists of a two-dimensional region manually drawn within the habenula as identified on this single axial slice of a T1-weighted series.

did not use any other waypoint or exclusion masks. This practice minimizes the number of user-dependent inputs, reducing the potential for bias due to over-constraining the tractography results based on preconceived notions of the course of the SM. We overlaid the colorized probabilistic tractograms on the original MPRAGE images for visualization. We adjusted their lower thresholds to a value equal to 1% of the product of the number of voxels contained within the seed mask and the number of tracts emanating from each voxel (5000 in this case), in order to display the full extent of the SM in all three orthogonal planes in a consistent manner.

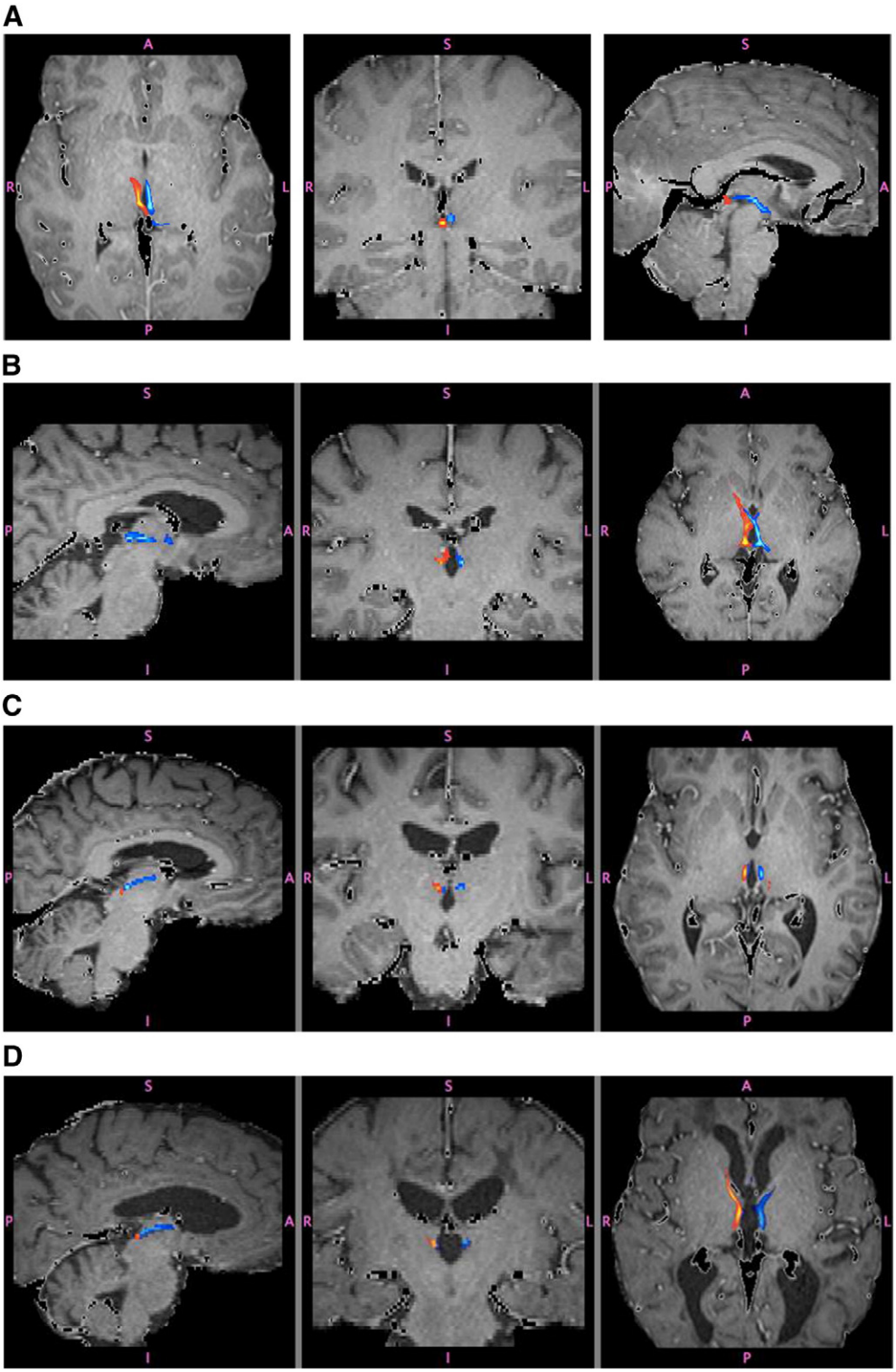

Fig. 2. Tractography results. The five subjects (A–E) are shown. Approximately 100,000 tracts were sent out, and the voxels shown in color have at least 1000 tracts traversing through them. The left SM is represented in blue while the right is represented in orange. (For interpretation of the references to color in this figure legend, the reader is referred to the web version of this article.)

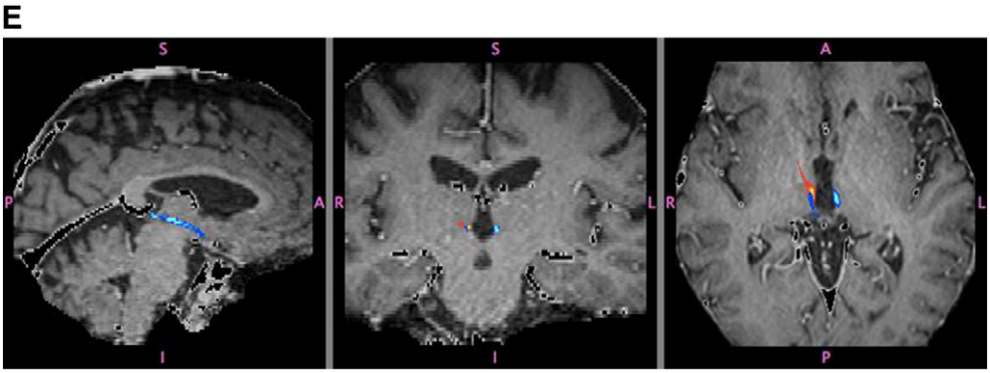

Fig. 2 (*continued*).

2.5. Variations in seed placement

Our current seed placement procedure requires manual identification of the axial slice in which the habenula is most visible, meaning there is potential for inter- and intra-operator differences in the slice chosen for seeding. Realistically, we expect these differences to be less than one slice. To understand the effect of such a deviation, we intentionally seeded the slice above and the slice below the central habenular slice and repeated the probabilistic tractography routine described above.

Single-voxel seeding is an alternative strategy that may be attractive to some users due to its simplicity. We demonstrated such an approach by drawing a one-voxel seed mask in ostensibly the most central location within the habenula and again repeating the tractography procedure described above.

3. Results

3.1. Visualization of the SM

In all five subjects, the SM was reliably visualized bilaterally using the above described technique of seeding the LHb (Fig. 2A–E). Roughly 100,000 tracts were sent out per LHb (5000 for each of about 20 seeded voxels), and the colorized voxels are those with at least 1000 tracts passing through them. Shades of blue represent the SM emanating from the left LHb while shades of orange emanate from the right.

3.2. Variations in choice of axial slice seeding

In all ten of the analyzed hemispheres, the LHb was clearly visible as a protrusion into the ventricle in typically three consecutive axial slices. Fig. 3 depicts tractograms (B) resulting from seed regions placed in the upper, middle, and lower slices (A), overlaid on a sagittal reformat of the T1-weighted series. Near their origin at the seed regions, the resulting tracts are noticeably divergent, with each individual tract coursing toward its respective seed. Moving anteriorly away from the seeds, the tracts begin to converge. Thus, in identifying the SM, the tractography exhibits some degree of stability with respect to small differences in the user-supplied seed location, and a 1.2-mm variation in seeding did not lead to wide deviations in course.

3.3. Seeding of a single voxel

A seed region consisting of a single voxel within the LHb leads to the SM tractogram depicted in Fig. 4. This tractogram is expectedly much

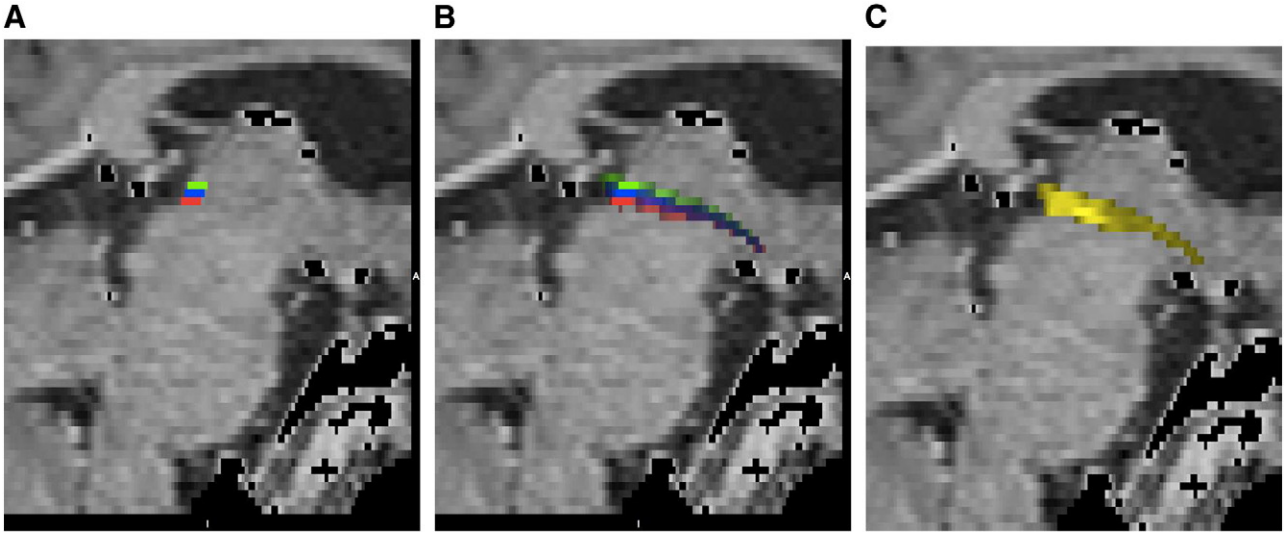

Fig. 3. Tractography based on axial seed slice. The habenula is visible as a protrusion into the ventricle in typically three consecutive axial slices as shown in green, blue, and red, respectively, in a sagittal reformat of the T1-weighted series (A). Note that these habenular seed regions are initially divergent; however, moving anteriorly away from the seeds, the tracts begin to converge (B). Creating a larger seed region spanning the three individual seed regions that lie in different axial planes has ultimately widened the region of uncertainty of the SM (C). (For interpretation of the references to color in this figure legend, the reader is referred to the web version of this article.)

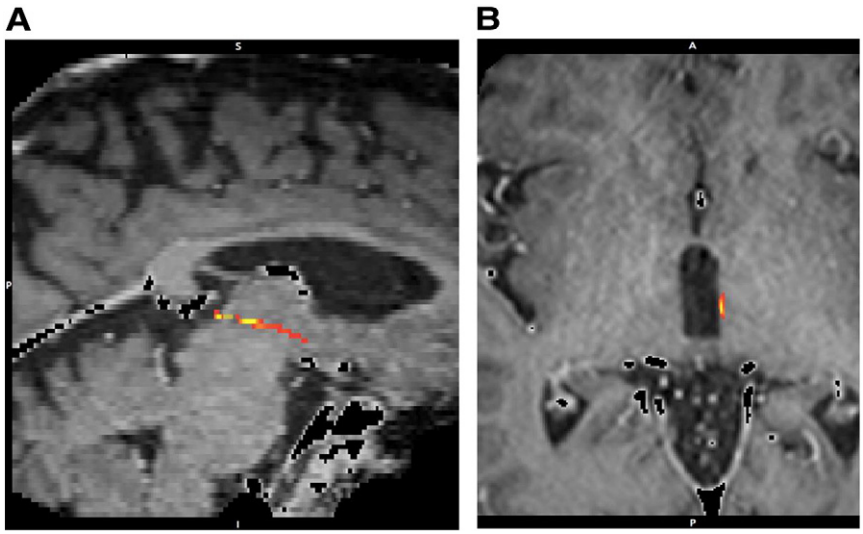

Fig. 4. Seeding a single voxel. This technique creates a tractogram much smaller in width on axial and sagittal series (A, B), and different selections of the single seed voxel are likely to give slightly varying tractography results. Thus, the single voxel seed approach may not give the most complete picture of the underlying SM anatomy.

narrower (just a voxel or so wide) but similar in anatomic course compared to those arising from two-dimensional multi-voxel seeds.

4. Discussion

Reported treatment efficacy of DBS for depression is highly variable with multiple targets described, none of which have shown to be significantly beneficial in randomized controlled trials (Dougherty et al., 2015). Therefore, efforts to identify the optimal target and stimulation parameters are ongoing. The use of DTI has heightened interest in stimulation of limbic system white matter tracts, in particular the slMFB, as it interconnects various centers of the reward pathway including the NAcc, ventral tegmental area (VTA), hypothalamus, and amygdala (Schoene-Bake et al., 2010). Rapid symptom improvement for TRD has been achieved in a series of six out of seven patients with stimulation of the slMFB (Schlaepfer et al., 2013). Efficacy of slMFB stimulation has also been shown to occur at lower stimulation parameters than structures such as the NAcc or VC/VS, and it has been hypothesized that the differences in required stimulation current are because the fiber tracts interconnecting psychiatric circuits are stimulated at varying distances and sections than grey matter structures (Coenen et al., 2009, 2011; Anthofer et al., 2015).

Given these observations and recent literature suggesting feasibility of DTI-based fiber tracking to characterize the MFB for DBS targeting, we sought to use DTI to define the stria medullaris thalami, another white matter tract implicated in the pathophysiology of TRD. DBS of the SM itself has yet to be described; however, stimulation of the LHb, the afferent projection of the SM has been reported in only two patients, albeit with promising results (Sartorius et al., 2010; Schneider et al., 2013). Given its multiple efferent connections to serotonergic, dopaminergic and noradrenergic centers, its proposed effect on treatment resistant depression is convincing; however, because of its small size and the inability for MRI to distinguish between medial habenula (MHb) and LHb, a trajectory across the entire habenular complex must be chosen to ensure stimulation of both the LHb and its afferent projection, the SM (Schneider et al., 2013). A high degree of targeting accuracy must therefore be ensured to avoid stimulation based side effects given its close proximity to midbrain structures like the superior colliculus. A trajectory analysis for LHb targeting by Schneider et al. demonstrated a need for a steep frontal trajectory in about half of the analyzed patients given the small size of the LHb and its proximity to critical structures like thalamic veins (Schneider et al., 2013). Although targeting of the LHb was shown to be feasible, a meticulously planned trajectory is paramount to avoid hemorrhagic complications from damage to thalamic veins or proximity to the ventricle (Schneider et al., 2013). Moreover, stimulation of the LHb in the one of the reported patients required a high voltage parameter (10.5 V) and a 4 month lag time to achieve clinical efficacy (Sartorius et al., 2010). Because of the compact size of the LHb and its proximity to critical brainstem structures like the collicular plate, targeting the anteriorly projecting afferent white matter pathway (SM) may not only provide a larger anatomic target but also reduce the stimulation voltages along with any associated side effects. Lastly, stimulation of the SM may also lead to more rapid onset symptom relief by extrapolating the previously described findings of slMFB stimulation. Recent literature has implicated the cortico-striatal-pallidal-thalamic loop in the pathophysiology of MDD which implies that stimulation of an afferent white matter tract like the SM modulates a node within a broad network involved in the pathophysiology of mood disorders (Downar et al., 2016).

We sought to demonstrate the utility of DTI based probabilistic fiber tracking to define a potentially broader target of the LHb through visualization of the SM. In all five patients, we were able to reliably visualize the SM bilaterally. Because we routinely perform the described DTI sequences in patients with Parkinson's disease (PD) prior to DBS surgery, these sequences were readily and easily accessible for the described study. There are no studies evaluating the visualization of SM in PD patients; however, disruption of the habenular-basal ganglia limbic cross pathways is likely affected neurochemically (Hikosaka et al., 2008). Given that the presented study is an anatomical one, and DTI is addressing the presence of the anatomical SM pathway, we feel that our radiographic findings can be extrapolated to the depression state. Our seeding strategy consisted of a two-dimensional region manually drawn within the habenula as identified on a single axial slice of a T1-weighted series. This T1, the MP-RAGE, was a routine 3D post-contrast series acquired for purposes of neuro-navigation, originally with 1 mm × 1 mm in-plane resolution but upsampled to 0.5 mm × 0.5 mm to allow more precise delineation of the small seed regions used for tractography. Susceptibility distortions of the raw diffusion-weighted data are fortuitously small in this region, and on top of this we carried out rigorous motion and distortion correction as described earlier. Therefore, we had high confidence that the habenular seed region as selected on the high resolution T1 actually corresponded to the same region on the diffusion-weighted series.

Importantly, we found that small differences in the chosen seed slice did not appear to significantly affect the course of the SM's trajectory. Thus, manual seeding, as opposed to atlas-based or automated seeding

via registration to a template, is likely an acceptable approach for tractography of the SM, though more advanced seeding strategies may be of interest in future investigations aimed at improving repeatability or streamlining the workflow. Similarly, the course of SM was relatively insensitive to whether the seed region consisted of a single voxel or multiple voxels. Thus, the single-voxel approach may serve as a viable simplification of the seeding procedure and may be preferred by some users. We note, however, that different selections of the single seed voxel will yield slightly different tractography results, as we demonstrated for the two-dimensional seed regions in Fig. 1, and this limitation of single-voxel seeding must be borne in mind. Conversely, a much larger seed region created by merging three individual seed regions that lie in different axial planes has the effect of widening the region of uncertainty for where the center of the SM might be truly located (Fig. 3C).

While the aim of our investigation was to define the SM using DTI so that it may ultimately be used for the purposes of direct targeting, it is important to note that while LHb stimulation has shown promise, no reports of direct stimulation of solely the SM have been reported. Thus, despite the theoretically promising effect of indirect LHb stimulation via the SM by extrapolating the findings of slMFB stimulation (i.e. potentially lower stimulation parameters through stimulation of white matter pathways, larger target area) the optimal stimulation location within the circuit has yet to be delineated.

One aspect of the current work that limits its immediate clinical relevance is the utilization of probabilistic tractography as opposed to deterministic tractography. To our knowledge, all tools approved for clinical use are based on deterministic tractography, the major advantages of which are speedier processing, nearly real-time rendering of new results for changes in the seed shape or location, and an intuitive manner of displaying those results (i.e. strings or tubes connecting one region to another). In the current work, we experimented with deterministic tractography but found its results to be at least slightly less stable and questionably accurate compared to the results of probabilistic tractography (see Supplement A). Thus, for the best chance of identifying the small bundle of white matter fibers that constitute the stria medullaris, we carried out the study using probabilistic tractography software that is unlikely to become a part of routine clinical workflow. Future work to define the utility of the more clinically accessible deterministic tractography in identification of the stria medullaris is therefore warranted, especially as processing techniques and algorithms improve.

5. Conclusion

We describe a reliable technique of defining the SM using MRI-based probabilistic tractography. Given the promising results of LHb stimulation for TRD, broader targeting of the LHb indirectly via the SM could provide a more anatomically favorable target.

Supplementary data to this article can be found online at http://dx.doi.org/10.1016/j.nicl.2016.10.018.

References

Anthofer, J.M., et al., 2015. DTI-based deterministic fibre tracking of the medial forebrain bundle. Acta Neurochir. 157, 469–477.

Behrens, T.E.J., Berg, H.J., Jbabdi, S., Rushworth, M.F.S., Woolrich, M.W., 2007. Probabilistic diffusion tractography with multiple fibre orientations: what can we gain? NeuroImage 34, 144–155.

Bewernick, B.H., Schlaepfer, T.E., 2013. Chronic depression as a model disease for cerebral aging. Dialogues Clin. Neurosci. 15, 77–85.

Coenen, V.A., et al., 2009. Medial forebrain bundle stimulation as a pathophysiological mechanism for hypomania in subthalamic nucleus deep brain stimulation for Parkinson's disease. Neurosurgery 64, 1106–1114 (discussion 1114–1115).

Coenen, V.A., Schlaepfer, T.E., Maedler, B., Panksepp, J., 2011. Cross-species affective functions of the medial forebrain bundle-implications for the treatment of affective pain and depression in humans. Neurosci. Biobehav. Rev. 35, 1971–1981.

Coenen, V.A., Panksepp, J., Hurwitz, T.A., Urbach, H., Mädler, B., 2012. Human medial forebrain bundle (MFB) and anterior thalamic radiation (ATR): imaging of two major subcortical pathways and the dynamic balance of opposite affects in understanding depression. J. Neuropsychiatr. Clin. Neurosci. 24, 223–236.

Dougherty, D.D., et al., 2015. A randomized sham-controlled trial of deep brain stimulation of the ventral capsule/ventral striatum for chronic treatment-resistant depression. Biol. Psychiatry 78, 240–248.

Downar, J., Blumberger, D.M., Daskalakis, Z.J., 2016. The neural crossroads of psychiatric illness: an emerging target for brain stimulation. Trends Cogn. Sci. 20, 107–120.

Hikosaka, O., Sesack, S.R., Lecourtier, L., Shepard, P.D., 2008. Habenula: crossroad between the basal ganglia and the limbic system. J. Neurosci. 28, 11825–11829.

Holtzheimer, P.E., et al., 2012. Subcallosal cingulate deep brain stimulation for treatment-resistant unipolar and bipolar depression. Arch. Gen. Psychiatry 69, 150–158.

Jenkinson, M., Beckmann, C.F., Behrens, T.E.J., Woolrich, M.W., Smith, S.M., 2012. FSL. NeuroImage 62, 782–790.

Jones, D.K., Horsfield, M.A., Simmons, A., 1999. Optimal strategies for measuring diffusion in anisotropic systems by magnetic resonance imaging. Magn. Reson. Med. 42, 515–525.

Lawson, R.P., Drevets, W.C., Roiser, J.P., 2013. Defining the habenula in human neuroimaging studies. NeuroImage 64, 722–727.

Lozano, A.M., et al., 2008. Subcallosal cingulate gyrus deep brain stimulation for treatment-resistant depression. Biol. Psychiatry 64, 461–467.

Malone, D.A., et al., 2009. Deep brain stimulation of the ventral capsule/ventral striatum for treatment-resistant depression. Biol. Psychiatry 65, 267–275.

Pierpaoli, C., et al., 2010. TORTOISE: An integrated software package for processing of diffusion MRI data. 18th Scientific Meeting of the International Society for Magnetic Resonance in Medicine, p. 1597.

Rorden, C., Karnath, H.-O., Bonilha, L., 2007. Improving lesion-symptom mapping. J. Cogn. Neurosci. 19, 1081–1088.

Sartorius, A., Henn, F.A., 2007. Deep brain stimulation of the lateral habenula in treatment resistant major depression. Med. Hypotheses 69, 1305–1308.

Sartorius, A., et al., 2010. Remission of major depression under deep brain stimulation of the lateral habenula in a therapy-refractory patient. Biol. Psychiatry 67, e9–e11.

Savitz, J.B., et al., 2011. Habenula volume in bipolar disorder and major depressive disorder: a high-resolution magnetic resonance imaging study. Biol. Psychiatry 69, 336–343.

Schlaepfer, T.E., Bewernick, B.H., Kayser, S., Mädler, B., Coenen, V.A., 2013. Rapid effects of deep brain stimulation for treatment-resistant major depression. Biol. Psychiatry 73, 1204–1212.

Schneider, T.M., Beynon, C., Sartorius, A., Unterberg, A.W., Kiening, K.L., 2013. Deep brain stimulation of the lateral habenular complex in treatment-resistant depression: traps and pitfalls of trajectory choice. Neurosurgery 72, ons184–ons193 (discussion ons193).

Schoene-Bake, J.-C., et al., 2010. Tractographic analysis of historical lesion surgery for depression. Neuropsychopharmacology. Off. Publ. Am. Coll. Neuropsychopharmacol. 35, 2553–2563.

Smith, S.M., 2002. Fast robust automated brain extraction. Hum. Brain Mapp. 17, 143–155.

Strotmann, B., et al., 2014. High-resolution MRI and diffusion-weighted imaging of the human habenula at 7 tesla. J. Magn. Reson. Imaging 39, 1018–1026.

Zhao, H., Zhang, B.-L., Yang, S.-J., Rusak, B., 2015. The role of lateral habenula-dorsal raphe nucleus circuits in higher brain functions and psychiatric illness. Behav. Brain Res. 277, 89–98.